12-1-2021

Enhanced drought resistance of vegetation growth in cities due to urban heat, CO2 domes and O3 troughs

Peng Fu
University of Illinois Urbana-Champaign

Leiqiu Hu
The University of Alabama in Huntsville

Elizabeth A. Ainsworth
University of Illinois Urbana-Champaign

Xiaonan Tai
New Jersey Institute of Technology

Soe W. Myint
Arizona State University

See next page for additional authors

Authors

Peng Fu, Leiqiu Hu, Elizabeth A. Ainsworth, Xiaonan Tai, Soe W. Myint, Wenfeng Zhan, Bethany J. Blakely, and Carl J. Bernacchi

LETTER • OPEN ACCESS

Enhanced drought resistance of vegetation growth in cities due to urban heat, CO_2 domes and O_3 troughs

To cite this article: Peng Fu *et al* 2021 *Environ. Res. Lett.* **16** 124052

View the article online for updates and enhancements.

ENVIRONMENTAL RESEARCH
LETTERS

LETTER

Enhanced drought resistance of vegetation growth in cities due to urban heat, CO$_2$ domes and O$_3$ troughs

Peng Fu[1,2,*] ⬤, Leiqiu Hu[3], Elizabeth A Ainsworth[1,2,4], Xiaonan Tai[5], Soe W Myint[6] ⬤, Wenfeng Zhan[7], Bethany J Blakely[1] and Carl J Bernacchi[1,2,4] ⬤

[1] Institute for Sustainability, Energy, and Environment, University of Illinois at Urbana-Champaign, Urbana, IL, 61801, United States of America
[2] Departments of Plant Biology and Crop Sciences, University of Illinois at Urbana-Champaign, Urbana, IL 61801, United States of America
[3] Department of Atmospheric and Earth Science, University of Alabama Huntsville in Huntsville, Huntsville, AL 35899, United States of America
[4] USDA ARS Global Change and Photosynthesis Research Unit, Urbana, IL 61801, United States of America
[5] Department of Biological Sciences, New Jersey Institute of Technology, Newark, NJ 07102, United States of America
[6] School of Geographical Sciences and Urban Planning, Arizona State University, Tempe, AZ 85281, United States of America
[7] Jiangsu Provincial Key Laboratory of Geographic Information Science and Technology, International Institute for Earth System Science, Nanjing University, Nanjing, Jiangsu 210023, People's Republic of China
* Author to whom any correspondence should be addressed.

E-mail: pengfu@illinois.edu

Abstract

Sustained increase in atmospheric CO$_2$ is strongly coupled with rising temperature and persistent droughts. While elevated CO$_2$ promotes photosynthesis and growth of vegetation, drier and warmer climate can potentially negate this benefit, complicating the prediction of future terrestrial carbon dynamics. Manipulative studies such as free air CO$_2$ enrichment (FACE) experiments have been useful for studying the joint effect of global change factors on vegetation growth; however, their results do not easily transfer to natural ecosystems partly due to their short-duration nature and limited consideration of climatic gradients and potential confounding factors, such as O$_3$. Urban environments serve as a useful small-scale analogy of future climate at least in reference to CO$_2$ and temperature enhancements. Here, we develop a data-driven approach using urban environments as test beds for revealing the joint effect of changing temperature and CO$_2$ on vegetation response to drought. Using 75 urban-rural paired plots from three climate zones over the conterminous United States (CONUS), we find vegetation in urban areas exhibits a much stronger resistance to drought than in rural areas. Statistical analysis suggests the drought resistance enhancement of urban vegetation across CONUS is attributed to rising temperature (with a partial correlation coefficient of 0.36) and CO$_2$ (with a partial correlation coefficient of 0.31) and reduced O$_3$ concentration (with a partial correlation coefficient of -0.12) in cities. The controlling factor(s) responsible for urban-rural differences in drought resistance of vegetation vary across climate regions, such as surface O$_3$ gradients in the arid climate, and surface CO$_2$ and O$_3$ gradients in the temperate and continental climates. Thus, our study provides new observational insights on the impacts of competing factors on vegetation growth at a large scale, and ultimately, helps reduce uncertainties in understanding terrestrial carbon dynamics.

1. Introduction

Terrestrial ecosystems assimilate *ca.* 30% of anthropogenic carbon dioxide (CO$_2$) emissions (Friedlingstein *et al* 2020) and have been a substantial carbon sink over the past six decades (Ballantyne *et al* 2012, Keenan and Williams 2018, Morecroft *et al* 2019). Increasing land carbon uptake has been partly attributed to enhanced vegetation growth in response to rising atmospheric CO$_2$ concentrations (Schimel *et al*

2015, Zhu *et al* 2016), known as the CO_2 fertilization effect. However, sustained global warming, coupled with extreme climate events such as droughts, have the potential to offset this CO_2 fertilization benefit, causing depressions in vegetation productivity and even a net release of CO_2 into the atmosphere (Lewis *et al* 2011, Choat *et al* 2018). Therefore, revealing the interactive and competing effects of altered temperature (ΔT) and CO_2 (ΔCO_2) on the response of vegetation growth and productivity to drought (D; hereafter denoted as $\Delta T \mid \Delta CO_2 \mid D$ effects) is critical for understanding terrestrial carbon cycle dynamics and for informing reliable mitigation and adaption plans for climate change (Reichstein *et al* 2013, Brodribb *et al* 2020).

Examining the $\Delta T \mid \Delta CO_2 \mid D$ effects on vegetation growth is generally challenging although there have been some manipulative experiments (Apgaua *et al* 2019, Birami *et al* 2020). With controlled experiments, there are uncertainties in translating experimental results into ecologically realistic predictions of how vegetation will respond to ΔT and ΔCO_2 under drought (Dusenge *et al* 2019, Brodribb *et al* 2020) at a large scale. In addition, the limited coverage of species and environmental conditions in manipulated experiments may result in inconclusive findings (Duan *et al* 2013, Birami *et al* 2020). For instance, ozone (O_3) exposure can induce reductions in vegetation growth (Gregg *et al* 2003, Ainsworth *et al* 2012) but is often overlooked in manipulative experiments. While large-scale free air CO_2 enrichment (FACE) and open top chambers experiments may allow exposure of vegetation to, besides rising CO_2, various stress factors such as drought and elevated temperature simultaneously (Ainsworth and Long 2021), such facilities are typically costly to maintain in the long term (Calfapietra *et al* 2010). It is also difficult in imposing more than two global change factors in these manipulative experiments. As such, there is a dearth of consistent long-term observations for advancing our knowledge of the interactive and combined effect of $\Delta T \mid \Delta CO_2 \mid D$ effects on vegetation growth. For example, stomatal closure in response to drought can result in low leaf intercellular CO_2 and an enhanced sensitivity of photosynthetic rate to rising atmospheric CO_2, i.e. 'the low intercellular CO_2 effect', thus leading to relatively larger carbon uptake under drought and elevated atmospheric CO_2 (Kelly *et al* 2016). This beneficial effect was demonstrated using two *Eucalyptus* species in short-term experiments where leaf area index remained unchanged while long-term acclimation to drought counteracted this benefit (Kelly *et al* 2016, Jiang *et al* 2021).

Here, we approach the interactive effects of environmental drivers on vegetation growth and productivity along an urban-rural gradient (Calfapietra *et al* 2015) from 2001 to 2018 in the conterminous United States (CONUS). This urban plant physiology concept advocates the use of urban-rural gradients

as a test bed and as a cost-efficient means for plant physiological studies since cities are experiencing conditions, such as temperature and CO_2 enhancements, decades ahead of projected change for natural ecosystems (Zhao *et al* 2016, Wang *et al* 2019). In addition, global climate change has exacerbated drought in both frequency and severity in urban and its neighboring rural regions (Güneralp *et al* 2015, Vicente-Serrano *et al* 2020), posing tremendous pressure on urban-rural ecosystems (Zhang *et al* 2019). With the long-term monitoring of drought conditions (Dai 2013, 2021), urban-rural contrasts in environmental conditions such as surface O_3 gradient (ΔO_3, typically higher O_3 concentrations in rural regions) can be exploited to reveal the response of vegetation growth and productivity to multiple altered environmental factors under drought. In this study, we analyze 75 urban-rural pairs of various sizes among three climatic zones (arid, temperate, and continental climate zones; figures 2, S1, and table S1 (available online at stacks.iop.org/ERL/16/124052/mmedia)) for revealing environmental drivers underlying ecosystem response to drought. The monthly enhanced vegetation index (EVI, 1 km) (Huete *et al* 2002) was used as a proxy for natural (non-crop) vegetation growth and productivity during the growing season, i.e. June, July, and August (JJA). EVI values were spatially averaged for urban and rural extents individually over pixels of plant functional types (PFTs) commonly identified in each urban-rural pair. We utilized a linear mixed-effects model to remove variation in EVI induced by climate variables such as solar radiation so that response of vegetation growth to drought and non-drought conditions could be inferred from EVI anomalies (i.e. observations—linear model predictions, denoted as EVI_a). Drought resistance of vegetation growth (ΔEVI_a) was computed as the difference in EVI_a between drought and non-drought conditions for each urban-rural pair. The objectives of this study are to reveal the urban-rural differences in drought resistance of vegetation growth (hereafter denoted as $dEVI_a$) and to understand the underlying drivers (e.g. irrigation) of such differences across the CONUS, particularly the role of ΔT, ΔO_3, and ΔCO_2, in explaining the observed $dEVI_a$ at a large scale.

2. Data and methods

2.1. Data for vegetation, weather, and drought

The monthly MODIS EVI Version 6 (MOD13 A3; https://lpdaac.usgs.gov/products/mod13a3v006/) data at 1 km were used as a proxy for vegetation growth and productivity. We only analyzed EVI derived during the growing season, i.e. JJA, between 2001 and 2018, because of the high-water demand from vegetation partly attributed to higher temperatures in summer relative to other seasons. The EVI product is computed from surface reflectance that

has been corrected for molecular scattering, ozone absorption, and aerosols. The EVI data are considered a better indicator than normalized difference vegetation index to characterize vegetation status in urban areas since EVI has improved sensitivity in high biomass regions and is less sensitive to canopy background signal and atmospheric influences (Huete *et al* 2002). In this study, urban extent and its rural counterpart each has a total of 54 observations, i.e. 18 (years) * 3 (months). Urban and rural extents were delineated using the yearly MODIS Land Cover Type (MCD12Q1; https://lpdaac.usgs.gov/products/mcd12q1v006/) Version 6 product (Sulla-Menashe *et al* 2019) (see details in supplementary document, Section-Delineation of urban and rural extents).

Gridded daily weather data are from the Daymet Version 4 product (Thornton *et al* 2020) (available at ORNL DACC https://https://daac.ornl.gov/cgi-bin/dsviewer.pl?ds_id=1840), including minimum temperature ($T_{\min}$), maximum temperature ($T_{\max}$), precipitation (Prcp), shortwave radiation (srad), and day length (dayl) at a spatial resolution of 1 km. The product is derived from daily meteorological observations recorded at weather stations in the North America and has undergone strict cross-validation and quality controls (Thornton *et al* 2021). srad and dayl were summarized into one variable as daily total radiation (Srad = srad * dayl). The daily weather variables were aggregated to monthly mean values from JJA between 2001 and 2018. Monthly PDSI dataset (Dai 2021) from the National Center for Atmospheric Research Climate Data Guide (https://climatedataguide.ucar.edu/climate-data/palmer-drought-severity-index-pdsi) is used to define dry to wet conditions for each urban-rural pair. PDSI is computed based on information associated with antecedent and current moisture supply (i.e. precipitation) and demand (i.e. potentiation evapotranspiration as a function of air temperature). It is a standardized metric with values typically ranging from −4 to 4 though further extreme values may be possible. The gridded product has a spatial resolution of 2.5° and thus each single urban-rural pair share one PDSI value. The single PDSI value can help understand the background drought conditions. We followed the NOAA Climate Prediction Center (www.cpc.ncep.noaa.gov/products/monitoring_and_data/drought.shtml) to define the drought conditions based on PDSI. Here a PDSI value less than −2 means that urban-rural pairs experience a drought condition and a value larger than 0 but less than 2 means that urban-rural pairs undergo a non-drought condition.

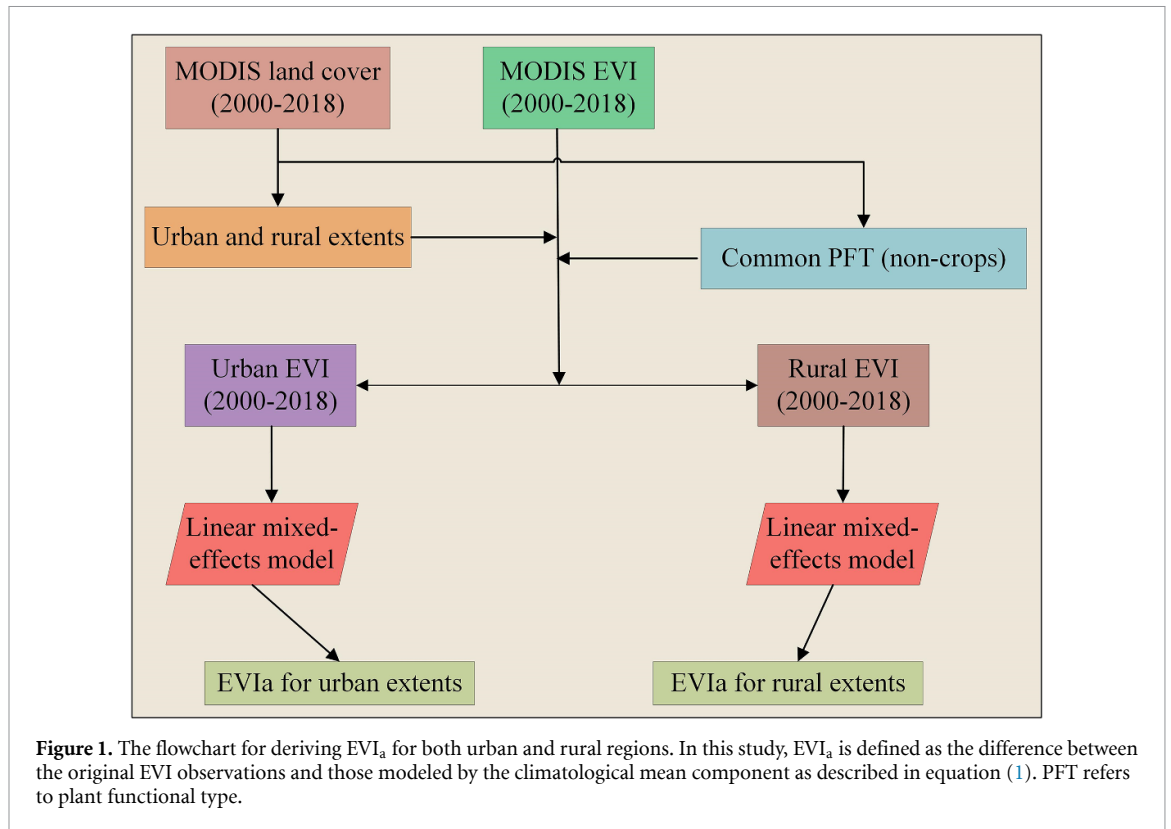## 2.2. Drought response of vegetation growth and productivity

Prior to the quantification of drought response of vegetation growth and productivity, common PFTs

were identified (further details related to identification of common PFTs can be found in supplementary section 2). Albeit the isolation of common PFTs within urban-rural pairs, EVI signals at 1 km still suffer background spectral contaminations from impervious surfaces or other non-vegetation pixels, resulting in smaller EVI values in urban extents compared to those in rural areas (Zhao *et al* 2016) with exceptions for urban-rural pairs in semi-arid and arid regions (Georgescu *et al* 2011) (figure S3). In addition, urban-rural differences in background climate can exert an impact on vegetation growth (i.e. EVI values).

Thus, direct comparisons in EVI between urban and rural areas (e.g. urban EVI minus rural EVI) under drought conditions (PDSI < −2) cannot facilitate revealing differences in drought response of vegetation growth and productivity between urban and rural areas. Here, a linear mixed-effects model was used to help define drought response of vegetation growth and productivity since the model did not have a strong requirement for data distribution (i.e. independent variables may not be necessarily normally distributed, Schielzeth *et al* (2020)). First, we conducted a panel analysis to remove variation in EVI induced by weather variables including $T_{\min}$, $T_{\max}$, Prcp, and Srad using equation (1) for all urban and all rural areas individually (thus urban-rural difference in climate variables can be accounted for):

$$y_{i,t} = \underbrace{\alpha_1 t + \alpha_2 T\min_{i,t} + \alpha_3 T\max_{i,t} + \alpha_4 \mathrm{Srad}_{i,t} + \alpha_5 \mathrm{Prcp}_{i,t}}_{\text{Climatologically mean}}$$
$$+ \underbrace{(1|\mathrm{City}_i)}_{\mathrm{EVI}_a} + \varepsilon_{i,t} \qquad (1)$$

where $y_{i,t}$ refers to EVI observations for city i in month t (June, July, or August) between 2001 and 2018, α_1 captures the EVI trend over the study period among cities, $\alpha_2, \alpha_3, \alpha_4, \alpha_5$ defines the sensitivity of EVI to $T_{\min}$, $T_{\max}$, Srad, and Prcp, respectively, $(1|\mathrm{City}_i)$ accounts for the random effect without intercept among cities (each city as a group), and ε is the error term. The component $(1|\mathrm{City}_i)$ can account for variations that do not change with climate variables, e.g. variations in EVI attributed to spatial variations of soil quality and impervious surface fractions among different cities and rural counterparts, respectively. Although each urban-rural pair shares one PDSI value extracted from the monthly PDSI dataset, there may be still differences in drought conditions between urban and rural regions. The weather variables including $T_{\min}$, $T_{\max}$, and Precp in equation (1) can help account for such differences in drought conditions between urban and rural regions that may not be captured by the monthly PDSI dataset. Baseline models without weather variables or random effects were also tested; however, both Akaike

Figure 1. The flowchart for deriving EVI_a for both urban and rural regions. In this study, EVI_a is defined as the difference between the original EVI observations and those modeled by the climatological mean component as described in equation (1). PFT refers to plant functional type.

information criterion and Bayesian information criterion values pointed to a better model as shown in equation (1).

In general, the grouped regression fitting through equation (1) provides a means to remove climate induced variation in EVI for each urban-rural pair and the model fitted values provided by $\alpha_1 - \alpha_5$ terms are assumed as climatologically mean EVI values. Then, we define the difference between original EVI observations and climatologically mean EVI values (i.e. original minus mean) as EVI_a (figure 1 shows the flowchart deriving EVI_a). Thus, the drought resistance/response of vegetation growth and productivity (represented as Δx_a) is defined using equation (2)

$$\Delta x_a = x_{a,d,l} - x_{a,nd,l}. \qquad (2)$$

where x is EVI, $x_{a,d}$ refers to EVI_a under drought conditions (PDSI < −2), $x_{a,nd}$ stands for EVI_a under non-drought conditions (0 < PDSI < 2), and l represent either urban or rural landscapes.

With equation (2), any city-specific effects such as soil quality and impervious fractions on vegetation status can be largely removed, which provides more confidence in comparing vegetation growth and productivity among the selected 75 cities. Equation (2) was applied to urban and rural extents separately (75*2*3 = 450 times). Droughts are expected to lower the vegetation productivity, and thus ΔEVI_a would be negative. A smaller reduction of EVI_a during major drought periods suggests a greater resistance of vegetation to the drought impact.

2.3. Urban-rural differences in environmental variables

To help explain the observed discrepancies in drought response of vegetation growth and productivity between urban and rural areas, variables associated with CO_2 and O_3 concentrations and mean temperature (T_m) were used. The mean temperatures for urban and rural extents individually were computed using T_{min} and T_{max} provided by the gridded Daymet product following equation (3):

$$T_{m,l} = (T_{max,l} + T_{min,l})/2 \qquad (3)$$

where l refers to either urban or rural extents. CO_2 concentrations within urban and rural extents were derived from the bias-corrected column-average dry air mole fraction of CO_2 (X_{CO_2}) from Orbiting Carbon Observatory (Eldering *et al* 2017) (OCO-2, spatial resolution 1.3*2.25 km^2). The X_{CO_2} dataset was obtained from the reprocessed OCO-2 Lite files Version 10 r (available at https://disc.gsfc.nasa.gov/datasets) and has a retrieval accuracy of approximately 1 ppm. Although X_{CO_2} is not a direct measurement of surface CO_2 concentration, the X_{CO_2} dataset well characterizes the urban CO_2 dome (if any) at the city level (Kort *et al* 2012, Fu *et al* 2019) and urban-rural gradients in X_{CO_2} have a linear relationship with surface CO_2 gradients (Wang *et al* 2019). Since the dataset is only available from 2014 and has large gaps in both spatial and temporal domains, the mean X_{CO_2} values were computed for urban and rural extents individually using all observations available within the urban or rural extents (i.e. X_{CO_2} values

between 2015 and 2019). Thus, we did not further differentiate variation in urban-rural X_{CO_2} gradients among JJA.

The ozone data were obtained using the hourly EPA's Air Quality Data (www.epa.gov/outdoor-air-quality-data) collected at outdoor monitors across the United States. Hourly O_3 data from each station within either an urban or rural polygon were aggregated to a monthly scale and then further averaged over all stations within that region (urban or rural). However, only around one-third of urban-rural pairs (24 of 75 urban-rural pairs) had valid monthly mean O_3 observations from 2001 to 2018, resulting in large data gaps for analysis. Thus, daily L2 total column O_3 data between 2004 and 2018 derived from the Ozone Monitoring Instrument (OMI) (Dobber *et al* 2006) onboard the Aura satellite (available at https://disc.gsfc.nasa.gov/datasets) were also used to facilitate surface-level O_3 estimations. The satellite based O_3 data were gridded at 0.25° by 0.25° and retrieved using the enhanced TOMS version-8 algorithm applied to the ultraviolet radiance data at 317.5 and 331.2 nm with a bias less than 3% (Balis *et al* 2007). We did not use the satellite based O_3 data directly for analysis in this study since the satellite O_3 dataset contained the total ozone column data. A regression analysis suggested that there was a statistically significant linear relationship between urban-rural differences in total column O_3 and surface O_3 gradients (equation (4)) (based on 24 urban-rural pairs, as shown in figure S5(C), with all three months of data considered). Thus, the regression equation was used to convert satellite based monthly mean O_3 differences between urban and rural areas to surface urban-rural differences in O_3. Behind this conversion, it was assumed that O_3 concentration was relatively stable over years for each month (either from satellite- or station-based observations). This assumption was evidenced by figures S5(A) and (B) showing that the ratio between standard deviation and mean of the O_3 concentration was relatively small (2%–10%) over years for each month within urban or rural extents.

The urban-rural differences in environmental variables (ΔE) including T_m, $X_{CO_2}(CO_2)$, and O_3 were calculated using equation (4):

$$\Delta E = E_u - E_r \tag{4}$$

where E indicates the variable T_m, CO_2, or O_3, E_u is the mean value in the urban extent, and E_r refers to the mean value in the rural region. To determine the main factors in controlling differences in drought response of vegetation growth and productivity, the partial correlations of Δx_a with latitude, longitude, urban size, mean monthly temperature, ΔT_m, ΔCO_2, and ΔO_3 were computed. We binned urban-rural differences in T_m, X_{CO_2}, and O_3 every 0.1 °C, 0.1 ppm, and 0.1 ppbv to reduce stochastic error and data

uncertainties. ΔT, ΔCO_2, ΔO_3 were also binned every 0.5 °C, 0.5 ppm, and 0.5 ppbv; however, the new binning strategy would not change the significant linear slopes as shown in figures 4(A)–(C).

3. Results

Drought resistance of vegetation growth and productivity in urban areas was stronger than drought resistance in rural areas based on analysis of monthly EVI from 2001 to 2018 (figure 2). Statistically significant differences (*p*-value < 0.05) were observed in ΔEVI_a between urban and rural areas except for urban-rural pairs in early summer in arid climate (figure 2). For all selected urban-rural pairs, on average, ΔEVI_a in urban areas, was less negative than that in rural areas regardless of months within the growing season (JJA) (figure 2(B)). These negative ΔEVI_a values are expected since ΔEVI_a refers to the difference in EVI_a between drought and non-drought conditions and mean EVI_a under drought is smaller than that under non-drought conditions (figure S4(B)). A less negative value in ΔEVI_a suggests a stronger ability to resist dampening effects of drought on vegetation growth. More specifically, mean ΔEVI_a in urban areas was -0.0435, -0.0261, and -0.0174, and in rural areas, was -0.0779, -0.0535, and -0.0316, for JJA, respectively (figure 2(B)). Intuitively, it may be reasonable to assume that the less negative mean ΔEVI_a value in urban areas stems from the fact that urban areas typically, except those in arid climate, exhibited a smaller EVI compared to rural regions in each month (JJA) (figure S3). The observed smaller EVI in urban areas in temperate and continental climate zones partly results from the coarse resolution of vegetated pixels (1 km) that suffer signal contaminations from underlying impervious surfaces (i.e. dampening effect of impervious surfaces on EVI). This mixed signal effects (or spectral mixture of vegetation and impervious surfaces within a pixel) can further propagate to EVI_a and ΔEVI_a calculations, causing smaller standard deviations in EVI_a (figure S4) and ΔEVI_a in urban regions compared to rural regions (figure 2). However, such an intuitive explanation should not be a concern since the ΔEVI_a was computed as the difference in EVI_a between drought and non-drought conditions for urban and rural extents individually (see the section 2 for further details), i.e. we did not compare EVI_a under drought conditions in urban areas with EVI_a under drought conditions in rural areas directly.

As regional climate largely controls the types of ecosystems, we further grouped urban-rural pairs into three main climate zones based on Köppen-Geiger scheme (Beck *et al* 2018), including arid, temperate, and continental climates. The drought resistance of vegetation growth within each climate zone is shown in figures 2(C)–(E). The separate analysis
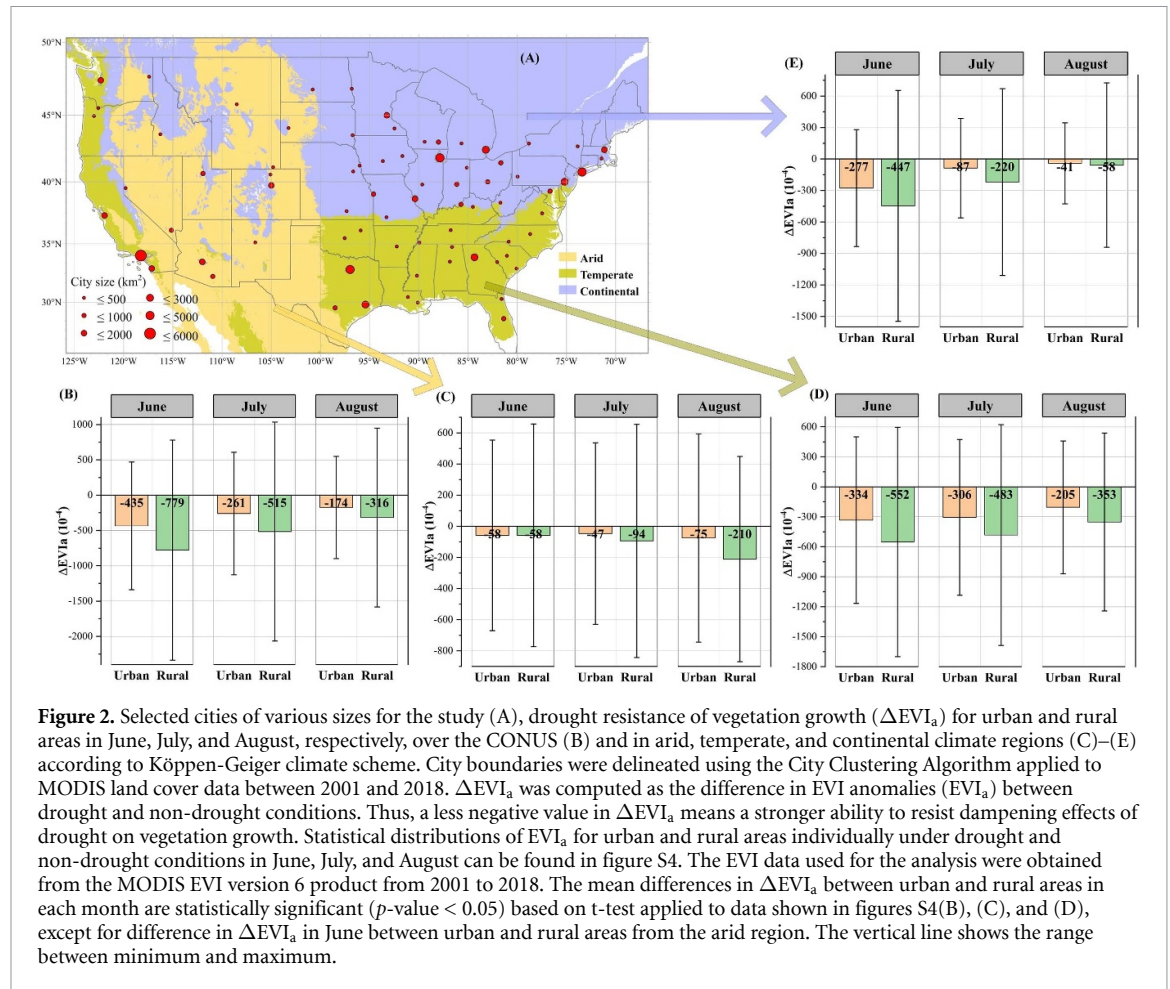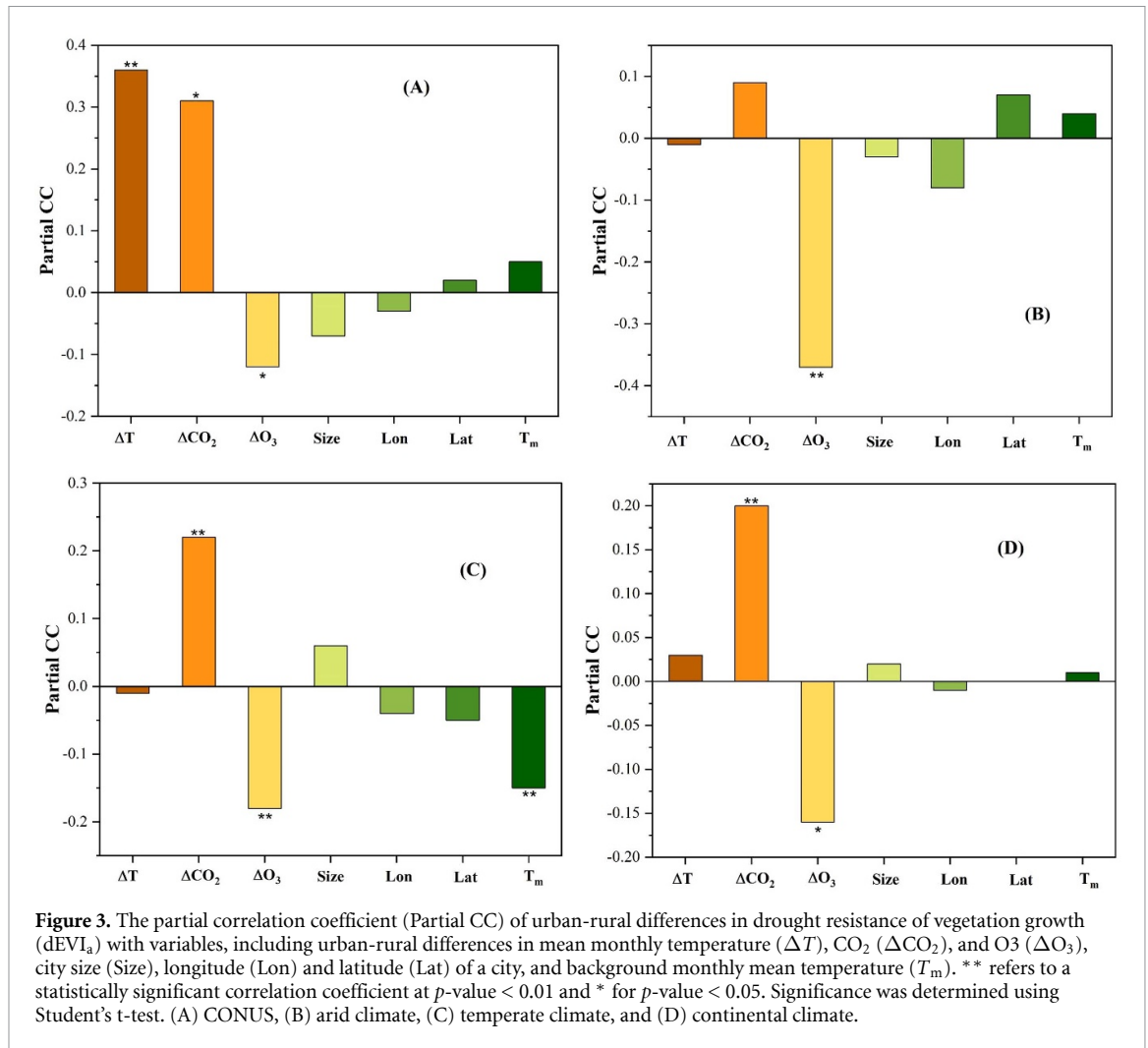
Figure 2. Selected cities of various sizes for the study (A), drought resistance of vegetation growth (ΔEVI_a) for urban and rural areas in June, July, and August, respectively, over the CONUS (B) and in arid, temperate, and continental climate regions (C)–(E) according to Köppen-Geiger climate scheme. City boundaries were delineated using the City Clustering Algorithm applied to MODIS land cover data between 2001 and 2018. ΔEVI_a was computed as the difference in EVI anomalies (EVI_a) between drought and non-drought conditions. Thus, a less negative value in ΔEVI_a means a stronger ability to resist dampening effects of drought on vegetation growth. Statistical distributions of EVI_a for urban and rural areas individually under drought and non-drought conditions in June, July, and August can be found in figure S4. The EVI data used for the analysis were obtained from the MODIS EVI version 6 product from 2001 to 2018. The mean differences in ΔEVI_a between urban and rural areas in each month are statistically significant (p-value < 0.05) based on t-test applied to data shown in figures S4(B), (C), and (D), except for difference in ΔEVI_a in June between urban and rural areas from the arid region. The vertical line shows the range between minimum and maximum.

among climate zones and months shows consistent findings that urban vegetation exhibits stronger ability to resist drought impacts than rural vegetation though the urban-rural differences in vegetation drought resistance varies (figures 2(C)–(E)). In the arid zone, on average, dEVI_a (urban-rural differences in drought resistance of vegetation growth) was 0.0047 and 0.0135 for July and August (p-value < 0.01), respectively while there was no difference in dEVI_a for June (p-value > 0.01). Compared to the arid zone, the temperate and continental climate zones in general showed a much higher value for dEVI_a in June and July. For example, the mean dEVI_a in July for urban-rural pairs under the continental climate was 0.0133 and under the temperate climate was 0.0177, much higher than 0.0047 for urban-rural pairs from the arid zone. For mean dEVI_a in August, urban-rural pairs from the temperate zone exhibited the largest value (0.0148), followed by those from the arid (0.0135) and continental (0.017) climate zones.

We next explored the potential effects of several drivers underlying urban-rural discrepancies in drought resistance of vegetation growth, including urban-rural differences in monthly mean temperature (ΔT), CO_2 (ΔCO_2), and O_3 (ΔO_3), city size (Size), the latitude and longitude of a city

(Lat and Lon, in case spatial location would be a factor), and background monthly mean temperature (T_m). To find the main factors controlling dEVI_a, partial correlation coefficients (partial CC) between dEVI_a and potential drivers were computed for all selected urban-rural pairs from all three climate zones (figure 3(A)) as well as separately for arid (figure 3(B)), temperate (figure 3(C)), and continental climates (figure 3(D)). The main factors in controlling dEVI_a across the conterminous U.S. were ΔT (partial CC of 0.36), ΔCO_2 (0.31), and ΔO_3 (-0.12) as seen in figure 3(A). Significant linear relations were also observed for the associations of ΔT, ΔCO_2, ΔO_3 and dEVI_a from binned observations (figure 4) that were adopted to reduce stochastic error and data uncertainties in the analysis. The main controlling factors for dEVI_a in each climate zone were different among three climate backgrounds. For example, the most influential variable was ΔO_3 in the arid zone (partial CC of 0.37, figure 3(B)), while in the temperate zone, the main drivers influencing dEVI_a were ΔCO_2 (partial CC of 0.22), ΔO_3 (partial CC of -0.18), and T_m (partial CC of -0.15) (figure 3(C)). In the continental zone (figure 3(D)), ΔCO_2, followed by ΔO_3 was the main factor in affecting dEVI_a. Overall, ΔT was identified as a main driver for dEVI_a over the CONUS

Figure 3. The partial correlation coefficient (Partial CC) of urban-rural differences in drought resistance of vegetation growth (dEVI$_a$) with variables, including urban-rural differences in mean monthly temperature (ΔT), CO$_2$ (ΔCO$_2$), and O3 (ΔO$_3$), city size (Size), longitude (Lon) and latitude (Lat) of a city, and background monthly mean temperature (T_m). ** refers to a statistically significant correlation coefficient at *p*-value < 0.01 and * for *p*-value < 0.05. Significance was determined using Student's t-test. (A) CONUS, (B) arid climate, (C) temperate climate, and (D) continental climate.
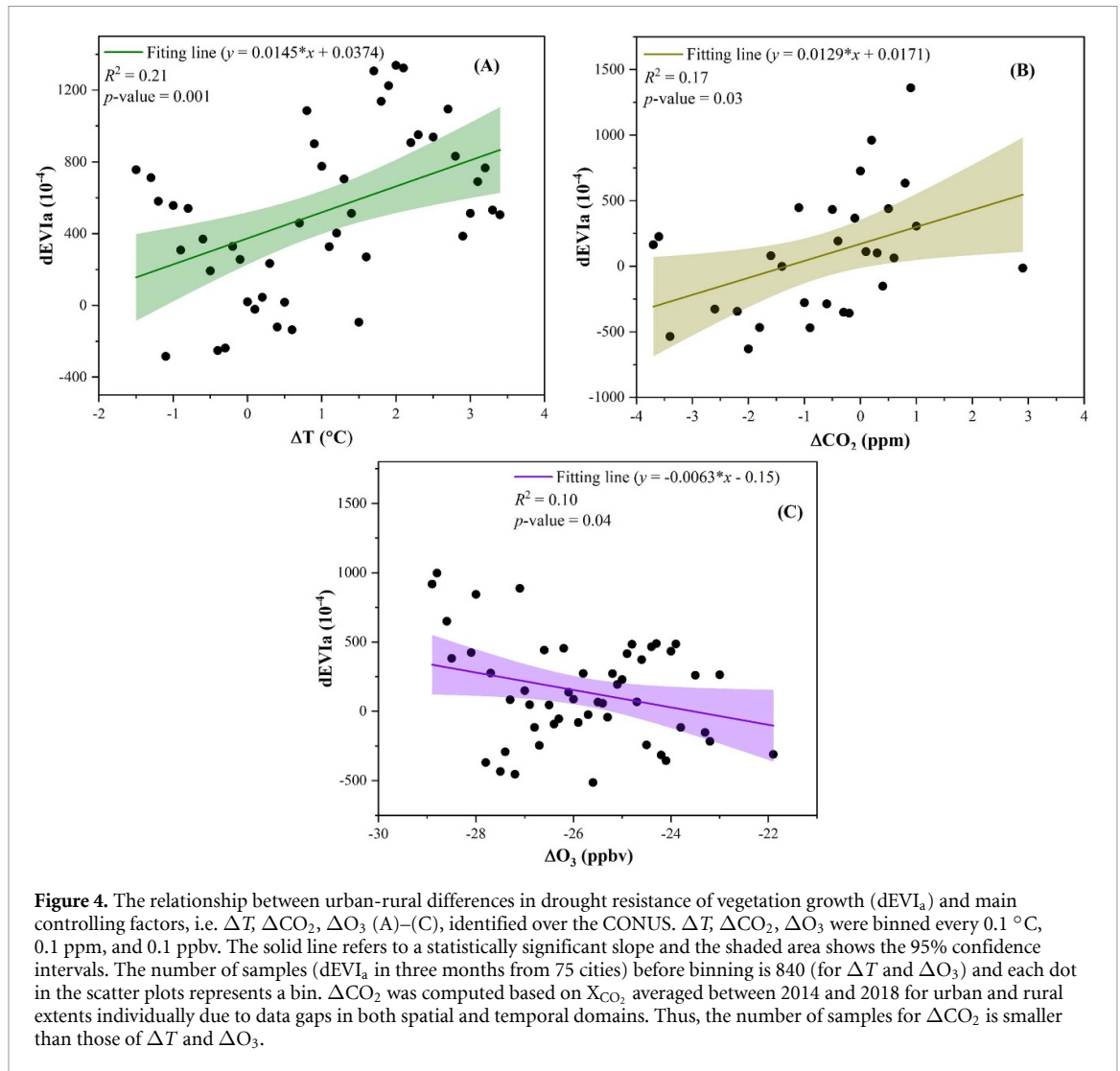
but not in each climate zone. Further explanations for this finding were presented in the discussion section.

4. Discussion and conclusions

We found urban ecosystems were more resistant to drought compared to their rural counterparts regardless of climate zones across CONUS. However, the main variables that contribute to such urban-rural differences in drought resistance of vegetation growth varies among climate zones. In general, surface temperature gradient (ΔT) was the most influential factor (*p*-value < 0.01, figure 2(A)) at the continental scale that consists of various ecosystems. Higher temperature in urban areas in relative to rural areas, observed for most of the selected urban-rural pairs (figure S6), likely leads to an earlier start but later end of the growing season and thus a longer growing season (Li *et al* 2017, Wang *et al* 2019), resulting in enhanced vegetation growth prevalent in urban areas (Zhao *et al* 2016) (while still a lower EVI value compared to rural areas due to the damping effect from impervious surfaces). Thus, when the very same drought occurred in both urban and rural

areas, the enhanced vegetation growth attributed to higher temperatures in urban areas exhibited a better ability/chance to endure/survive drought stress. In addition, plants growing in warmer/drier urban environments may already have had (screened before planting) or developed traits that allow them to better cope with drought stress (Anderegg and HilleRis-Lambers 2016). However, ΔT was not the controlling factor driving the urban-rural contrast of vegetation drought resistance within individual climate zones as shown in figure 3 partly due to the much less variation of ΔT in each climate zone (figure S7). Specifically, as shown in figure S7, vegetation growth in arid or semi-arid cities in general exhibits a much stronger drought resistance compared to that in the other two climate zones despite a wide range of ΔT from −2.0 °C to 3.5 °C. Even though urban-rural difference in drought resistance varies from −0.10 to 0.11 within temperate or continental climate regions, in a similar magnitude of variation in arid climate, there is a much smaller variation of ΔT. Thus, the urban-rural temperature gradient is not strong enough to cause such considerable differences in vegetation growth. The stronger drought resistance of vegetation (mainly shrub and grass) growth in cities from the arid zone

Figure 4. The relationship between urban-rural differences in drought resistance of vegetation growth (dEVI$_a$) and main controlling factors, i.e. ΔT, ΔCO_2, ΔO_3 (A)–(C), identified over the CONUS. ΔT, ΔCO_2, ΔO_3 were binned every 0.1 °C, 0.1 ppm, and 0.1 ppbv. The solid line refers to a statistically significant slope and the shaded area shows the 95% confidence intervals. The number of samples (dEVI$_a$ in three months from 75 cities) before binning is 840 (for ΔT and ΔO_3) and each dot in the scatter plots represents a bin. ΔCO_2 was computed based on X_{CO_2} averaged between 2014 and 2018 for urban and rural extents individually due to data gaps in both spatial and temporal domains. Thus, the number of samples for ΔCO_2 is smaller than those of ΔT and ΔO_3.

was mainly related to vegetation growth in rural areas exposed to higher ozone concentration (figure S8). Higher ozone concentration in rural areas than in cities (Gregg *et al* 2003), could cause more reduction in photosynthesis and vegetation growth in rural areas (Ainsworth *et al* 2012), which accounted for the negative relationship between surface O_3 gradients and urban-rural differences in drought resistance of vegetation growth (figures 3 and 4(C)). In addition, urban-rural difference in drought resistance of vegetation growth in the temperate zone is also sensitive to background monthly mean temperature T_m. Since the selected urban-rural pairs from the temperate climate zone exhibits the highest background monthly mean temperature (figure S9), this result emphasizes possible temperature stress on vegetation growth, particularly in urban areas, given relatively stable temperature gradients for urban-rural pairs from the temperate zone (figure S7).

Surface CO_2 gradient is identified as another important factor, in addition to surface temperature and O_3 gradients, responsible for the observed urban-rural discrepancies in drought resistance of vegetation growth. The surface CO_2 gradient is represented by the satellite-based X_{CO_2} gradient since there is a positive, linear relationship between the two (with a scale factor of ∼25) (Wang *et al* 2019). This satellite-based CO_2 gradient dataset (figure S10) shows that a greater difference in CO_2 concentration between urban and rural areas could result in a much stronger urban-rural difference in drought resistance of vegetation growth, particularly under temperate and continental climates (figures 3(A), (C), (D) and 4(B)). This conclusion is consistent with previous studies that emphasize the beneficial effect of atmospheric CO_2 enhancement on vegetation growth under drought conditions by stimulating photosynthesis (Ainsworth and Rogers 2007) or by increasing the water use efficiency of plants (Keenan *et al* 2013). However, the beneficial effect of CO_2 on urban-rural contrast in drought resistance is observed in temperate and continental zones rather than in arid zones even though urban-rural pairs from the arid zone typically showed the largest CO_2 gradient (figure S11). The insensitivity of drought impact on vegetation growth to CO_2 gradients in the arid zone, relative to

other two climate zones, may result from other more limiting factors such as nutrient deficiency (Wang *et al* 2020) or stomatal closure in response to rising CO_2 at the cost of enhanced growth (Frank *et al* 2015) in urban regions from the arid zone. Drought in the water-limited region is often more severe (as indicated in figure S12), and it is also possible that such drought condition completely overwhelms the beneficial effects of elevated CO_2 on vegetation growth.

Despite the identified main variables, factors such as landscape configuration/composition, atmospheric deposition (e.g. nitrogen and phosphorus), and management practices may also affect the observed discrepancies in drought resistance of vegetation growth between urban and rural areas. For example, urban landscape configuration and composition has been related to surface temperature gradients between urban and rural areas (Connors *et al* 2013, Estoque *et al* 2017), thus either strengthening or accentuating the effect of temperature gradients on difference in drought resistance between urban and rural vegetation growth. As urban areas typically have a higher atmospheric nitrogen and phosphorus deposition (Decina *et al* 2018), this may lessen nutrient restrictions on vegetation growth, thus contributing positively to the observed differences in drought resistance of vegetation growth between urban and rural areas. Human practices such as urban irrigation, however, may be a factor weakening the conclusion made towards the main factors driving the urban-rural differences in drought resistance of vegetation growth. Thus, we repeated the analysis by excluding some urban-rural pairs from the arid zone where irrigation typically was most pronounced and led to 'the oasis effect' (Georgescu *et al* 2011), i.e. higher EVI in cities than in rural areas (figure S3). Further analysis of urban-rural pairs from the three climate zones suggests that the main factors controlling the urban-rural differences in drought resistance of vegetation growth are still gradients of temperature and CO_2 and O_3 concentrations but with a smaller partial CC (figures S13 and 3(A)). Thus, although urban irrigation contributed positively to the observed urban-rural contrasts in drought resistance of vegetation growth, such a factor alone could not explain all the observed variances associated with drought resistance. Even under strong irrigation for cities in the arid zone, surface O_3 gradient was still identified as the main driver for observed discrepancies in drought resistance of vegetation growth between urban and rural areas (figure 3(B)). As such, there is strong evidence in attributing the observed discrepancies in drought resistance of vegetation growth between urban and rural areas to factors including temperature, CO_2, and O_3 gradients. Urban-rural gradients in wind speed and humidity were also accounted for in the analysis

(figure S15). The results suggested the controlling factor for the urban-rural differences in drought resistance would still be temperature, CO_2, and O_3 gradients (figure S15).

Benefiting from long-term satellite and station-based datasets, our study provides a data driven approach for revealing the impacts of competing and interactive environmental factors on response of vegetation growth to drought at a large scale. This approach advocates the urban plant physiology concept by utilizing urban-rural contrasts in environmental conditions, such as altered temperature gradients and O_3 concentration. The substantial differences in environmental conditions along urban-rural gradients can provide a 'natural laboratory' that is more widely accessible, compared to manipulative environments, to the scientific community to understand ecosystem traits under a changing climate. With projected increase in temperature and atmospheric CO_2 in the future, we can also select only urban-rural pairs with positive values in ΔT and ΔCO_2 for analysis. In this case, it is found that the mean urban-rural difference in drought resistance of vegetation growth becomes positive, i.e. 0.0389 for June, 0.0294 for July, and 0.0201 for August (figure S14). Thus, the novel aspect of this study is to provide a more general assessment of vegetation responses to environmental factors across different regions, and ultimately, to reduce uncertainties in quantifying terrestrial carbon dynamics.

Data availability statement

All data that support the findings of this study are included within the article (and any supplementary files).

Acknowledgments

comments and suggestions which helped improve this manuscript.

Conflict of interest

The authors declare no conflicts of interest relevant to this study.

ORCID iDs

Peng Fu ⬤ https://orcid.org/0000-0003-1568-1518
Soe W Myint ⬤ https://orcid.org/0000-0001-7809-1211
Carl J Bernacchi ⬤ https://orcid.org/0000-0002-2397-425X

References

Ainsworth E A and Long S P 2021 30 years of free-air carbon dioxide enrichment (FACE): what have we learned about future crop productivity and its potential for adaptation? *Global Change Biol.* **27** 27–49

Ainsworth E A and Rogers A 2007 The response of photosynthesis and stomatal conductance to rising [CO_2]: mechanisms and environmental interactions *Plant Cell Environ.* **30** 258–70

Ainsworth E A, Yendrek C R, Sitch S, Collins W J and Emberson L D 2012 The effects of tropospheric ozone on net primary productivity and implications for climate change *Annu. Rev. Plant Biol.* **63** 637–61

Anderegg L D L and HilleRisLambers J 2016 Drought stress limits the geographic ranges of two tree species via different physiological mechanisms *Global Change Biol.* **22** 1029–45

Apgaua D M G, Tng D Y P, Forbes S J, Ishida Y F, Vogado N O, Cernusak L A and Laurance S G W 2019 Elevated temperature and CO_2 cause differential growth stimulation and drought survival responses in eucalypt species from contrasting habitats *Tree Physiol.* **39** 1806–20

Balis D, Kroon M, Koukouli M E, Brinksma E J, Labow G, Veefkind J P and McPeters R D 2007 Validation of Ozone Monitoring Instrument total ozone column measurements using Brewer and Dobson spectrophotometer ground-based observations *J. Geophys. Res. Atmos.* **112** D24S46

Ballantyne A P, Alden C B, Miller J B, Tans P P and White J W C 2012 Increase in observed net carbon dioxide uptake by land and oceans during the past 50 years *Nature* **488** 70–72

Beck H E, Zimmermann N E, McVicar T R, Vergopolan N, Berg A and Wood E F 2018 Present and future Köppen-Geiger climate classification maps at 1-km resolution *Sci. Data* **5** 180214

Birami B, Nägele T, Gattmann M, Preisler Y, Gast A, Arneth A and Ruehr N K 2020 Hot drought reduces the effects of elevated CO_2 on tree water-use efficiency and carbon metabolism *New Phytol.* **226** 1607–21

Brodribb T J, Powers J, Cochard H and Choat B 2020 Hanging by a thread? Forests and drought *Science* **368** 261

Calfapietra C *et al* 2010 Challenges in elevated CO_2 experiments on forests *Trends Plant Sci.* **15** 5–10

Calfapietra C, Peñuelas J and Niinemets Ü 2015 Urban plant physiology: adaptation-mitigation strategies under permanent stress *Trends Plant Sci.* **20** 72–75

Choat B, Brodribb T J, Brodersen C R, Duursma R A, López R and Medlyn B E 2018 Triggers of tree mortality under drought *Nature* **558** 531–9

Connors J P, Galletti C S and Chow W T L 2013 Landscape configuration and urban heat island effects: assessing the relationship between landscape characteristics and land surface temperature in Phoenix, Arizona *Landscape Ecol.* **28** 271–83

Dai A 2013 Increasing drought under global warming in observations and models *Nat. Clim. Change* **3** 52–58

Dai A 2021 Hydroclimatic trends during 1950–2018 over global land *Clim. Dyn.* **56** 4027–49

Decina S M, Templer P H and Hutyra L R 2018 Atmospheric inputs of nitrogen, carbon, and phosphorus across an urban area: unaccounted fluxes and canopy influences *Earth's Future* **6** 134–48

Dobber M R *et al* 2006 Ozone monitoring instrument calibration *IEEE Trans. Geosci. Remote Sens.* **44** 1209–38

Duan H, Amthor J S, Duursma R A, O'Grady A P, Choat B and Tissue D T 2013 Carbon dynamics of eucalypt seedlings exposed to progressive drought in elevated [CO_2] and elevated temperature *Tree Physiol.* **33** 779–92

Dusenge M E, Duarte A G and Way D A 2019 Plant carbon metabolism and climate change: elevated CO_2 and temperature impacts on photosynthesis, photorespiration and respiration *New Phytol.* **221** 32–49

Eldering A *et al* 2017 The orbiting carbon observatory-2 early science investigations of regional carbon dioxide fluxes *Science* **358** eaam5745

Estoque R C, Murayama Y and Myint S W 2017 Effects of landscape composition and pattern on land surface temperature: an urban heat island study in the megacities of Southeast Asia *Sci. Total Environ.* **577** 349–59

Frank D C *et al* 2015 Water-use efficiency and transpiration across European forests during the Anthropocene *Nat. Clim. Change* **5** 579–83

Friedlingstein P *et al* 2020 Global carbon budget 2020 *Earth Syst. Sci. Data* **12** 3269–340

Fu P, Xie Y, Moore C E, Myint S W and Bernacchi C J 2019 A comparative analysis of anthropogenic CO_2 emissions at city level using OCO-2 observations: a global perspective *Earth's Future* **7** 1058–70

Georgescu M, Moustaoui M, Mahalov A and Dudhia J 2011 An alternative explanation of the semiarid urban area 'oasis effect' *J. Geophys. Res. Atmos.* **116** D24113

Gregg J W, Jones C G and Dawson T E 2003 Urbanization effects on tree growth in the vicinity of New York City *Nature* **424** 183–7

Güneralp B, Güneralp İ and Liu Y 2015 Changing global patterns of urban exposure to flood and drought hazards *Glob. Environ. Change* **31** 217–25

Huete A, Didan K, Miura T, Rodriguez E P, Gao X and Ferreira L G 2002 Overview of the radiometric and biophysical performance of the MODIS vegetation indices *Remote Sens. Environ.* **83** 195–213

Jiang M, Kelly J W G, Atwell B J, Tissue D T and Medlyn B E 2021 Drought by CO_2 interactions in trees: a test of the water savings mechanism *New Phytol.* **230** 1421–34

Keenan T F, Hollinger D Y, Bohrer G, Dragoni D, Munger J W, Schmid H P and Richardson A D 2013 Increase in forest water-use efficiency as atmospheric carbon dioxide concentrations rise *Nature* **499** 324–7

Keenan T F and Williams C A 2018 The terrestrial carbon sink *Annu. Rev. Environ. Resour.* **43** 219–43

Kelly J W G, Duursma R A, Atwell B J, Tissue D T and Medlyn B E 2016 Drought × CO_2 interactions in trees: a test of the low-intercellular CO_2 concentration (Ci) mechanism *New Phytol.* **209** 1600–12

Kort E A, Frankenberg C, Miller C E and Oda T 2012 Space-based observations of megacity carbon dioxide *Geophys. Res. Lett.* **39** L17806

Lewis S L, Brando P M, Phillips O L, van der Heijden G M F and Nepstad D 2011 The 2010 Amazon Drought *Science* **331** 554

Li X, Zhou Y, Asrar G R, Mao J, Li X and Li W 2017 Response of vegetation phenology to urbanization in the conterminous United States *Global Change Biol.* **23** 2818–30

Morecroft M D, Duffield S, Harley M, Pearce-Higgins J W, Stevens N, Watts O and Whitaker J 2019 Measuring the

success of climate change adaptation and mitigation in
terrestrial ecosystems *Science* **366** eaaw9256

Reichstein M *et al* 2013 Climate extremes and the carbon cycle
Nature **500** 287–95

Schielzeth H *et al* 2020 Robustness of linear mixed-effects models
to violations of distributional assumptions *Methods Ecol.
Evol.* **11** 1141–52

Schimel D, Stephens B B and Fisher J B 2015 Effect of increasing
CO_2 on the terrestrial carbon cycle *Proc. Natl Acad. Sci.*
112 436

Sulla-Menashe D, Gray J M, Abercrombie S P and Friedl M A
2019 Hierarchical mapping of annual global land cover 2001
to present: the MODIS collection 6 land cover product
Remote Sens. Environ. **222** 183–94

Thornton M M, Shrestha R, Wei Y, Thornton P E, Kao S-C and
Wilson B E 2020 Daymet: daily surface weather data on a
1-km grid for North America, version 4 *ORNL DAAC* (Oak
Ridge, Tennessee, USA)

Thornton P E, Shrestha R, Thornton M, Kao S-C, Wei Y and
Wilson B E 2021 Gridded daily weather data for North

America with comprehensive uncertainty quantification—
Daymet version 4 *Sci. Data* **8** 190

Vicente-Serrano S M, Quiring S M, Peña-Gallardo M, Yuan S and
Domínguez-Castro F 2020 A review of environmental
droughts: increased risk under global warming? *Earth-Sci.
Rev.* **201** 102953

Wang S *et al* 2019 Urban−rural gradients reveal joint control of
elevated CO_2 and temperature on extended photosynthetic
seasons *Nat. Ecol. Evol.* **3** 1076–85

Wang S *et al* 2020 Recent global decline of CO_2 fertilization
effects on vegetation photosynthesis *Science*
370 1295

Zhang X *et al* 2019 Urban drought challenge to 2030
sustainable development goals *Sci. Total Environ.*
693 133536

Zhao S, Liu S and Zhou D 2016 Prevalent vegetation growth
enhancement in urban environment *Proc. Natl Acad. Sci.*
113 6313

Zhu Z *et al* 2016 Greening of the Earth and its drivers *Nat. Clim.
Change* **6** 791–5